IV.C.9 Improving the Kinetics and Thermodynamics of $Mg(BH_4)_2$ for Hydrogen Storage

Brandon Wood (Primary Contact),
Lennie Klebanoff, Vitalie Stavila, Tae Wook Heo,
Keith Ray, Jonathan Lee, Hui-Chia Yu,
Katsuyo Thornton
Lawrence Livermore National Laboratory (LLNL)
7000 East Ave., L-413
Livermore, CA 94550
Phone: (925) 422-8391
Email: brandonwood@llnl.gov

DOE Manager
Jesse Adams
Phone: (720) 356-1421
Email: Jesse.Adams@ee.doe.gov

Subcontractors
- Sandia National Laboratories, Livermore, CA
- University of Michigan, Ann Arbor, MI

Project Start Date: August 1, 2014
Project End Date: August 31, 2017

Overall Objectives

- Combine theory, synthesis, and characterization across multiple scales to understand the intrinsic kinetic and thermodynamic limitations in $MgB_2/Mg(BH_4)_2$
- Construct and apply a flexible, validated, multiscale theoretical framework for modeling (de)hydrogenation kinetics of the Mg-B-H system and related metal hydrides
- Devise strategies for improving kinetics and thermodynamics through nanostructuring and doping

Fiscal Year (FY) 2015 Objectives

- Synthesize and characterize high-purity MgB_2 and $Mg(BH_4)_2$ materials
- Measure hydrogenation kinetics of bulk MgB_2 and examine phase composition
- Establish and calibrate initial modeling framework and test computational feasibility

Technical Barriers

This project addresses the following technical barriers from the Hydrogen Storage section of the Fuel Cell Technologies Office Multi-Year Research, Development, and Demonstration Plan:

(O) Lack of Understanding of Hydrogen Physisorption and Chemisorption

(A) System Weight and Volume

(E) Charging/Discharging Rates

Technical Targets

This project is conducting fundamental studies of hydrogenation and dehydrogenation of nanoscale $Mg(BH_4)_2$-based materials using a combined theory/experiment approach. Insights will be applied toward the design and synthesis of hydrogen storage materials that meet the following DOE hydrogen storage targets:

- Specific energy: 1.8 kWh/kg
- Energy density: 1.3 kWh/L
- Minimum delivery pressure: 5 bar
- Minimum delivery temperature: 85°C
- System fill time: 1.5 kg H_2/min

FY 2015 Accomplishments

- Synthesized high-purity MgB_2 and $Mg(BH_4)_2$ materials
- Performed measurements of bulk MgB_2 hydrogenation kinetics
- Performed nuclear magnetic resonance (NMR) and X-ray absorption (XAS)/X-ray emission (XES) of pristine and partially hydrogenated bulk MgB_2
- Established initial modeling framework to predict phase fractions, accounting for (1) thermodynamics of interfaces, surfaces, and bulk; (2) elastic effects and mechanical stress/strain; and (3) phase nucleation/evolution and non-equilibrium (de)hydrogenation
- Completed initial calculations of thermodynamic parameters for bulk and surface MgB_2-$Mg(BH_4)_2$
- Tested computational feasibility of phase fraction prediction code on Li-N-H system to successfully explain observed changes in reaction pathways with nanoconfinement

✧ ✧ ✧ ✧ ✧

INTRODUCTION

$Mg(BH_4)_2$ is one of very few metal hydride candidates that lie close to the "viability window" of capacity (14.9 wt% H) and desorption enthalpy (ΔH_{des}) required to satisfy the 2020 and ultimate DOE hydrogen storage targets [1–2]. However, $Mg(BH_4)_2$ suffers from extremely poor kinetics whose origin is not well understood. If the kinetic limitations could be removed and the effective ΔH_{des} slightly improved, then facile hydrogen uptake and release could be attained, and a complex metal hydride-based system could achieve long-term targets. Prior work points to particle size reduction and doping with additives as viable and cost effective improvement strategies [3]. However, it is difficult to fully leverage these without comprehending how, why, and under what conditions these improvements are observed. This project applies multiscale theoretical and experimental tools to develop a fundamental understanding of kinetic and thermodynamic limitations in the Mg-B-H hydrogen storage system, and to devise specific strategies for optimizing its performance under cycling conditions.

APPROACH

This project aims to establish a closely coupled theory/characterization/synthesis approach to understand the roles of nanostructuring and doping in the Mg-B-H system, and apply it to devise possible strategies for improving kinetics and thermodynamics. We focus on three objectives, (1) determining whether chemical, phase nucleation, or transport processes are rate limiting; (2) understanding the origin of the kinetic/thermodynamic changes upon nanosizing/doping; and (3) devising and implementing rational modifications for improvement of H_2 storage properties. Our modeling effort relies on the application of a multiscale framework that combines atomistic density functional theory (DFT) for predictive chemistry and thermodynamics with continuum phase-field modeling (PFM) for describing phase nucleation/growth and non-equilibrium transport kinetics. The predictions are informed and validated by controlled synthesis of size-selected nanoparticles free from binders and nanoscaffolds that may otherwise burden the system with unacceptably high gravimetric penalties. To better understand the kinetic pathways and processes, we apply gravimetric and thermochemical analysis, and utilize in situ and ex situ microscopic and spectroscopic characterization to derive chemical and phase compositions.

RESULTS

Experimental: To provide the large amount of high-quality $Mg(BH_4)_2$ and MgB_2 needed for the bulk hydrogenation kinetic and reaction pathway measurements, we developed synthetic methods for isolating phase-pure $Mg(BH_4)_2$ and MgB_2 with purities exceeding that available from commercial sources. $Mg(BH_4)_2$ was synthesized using a wet-chemistry approach involving the reaction of dibutylmagnesium with borane-dimethylsulfide (BH_3-SMe_2) in a heptane/toluene solution to form a dimethylsulfide adduct of magnesium borohydride, $Mg(BH_4)_2(SMe_2)_2$, which was converted to γ-$Mg(BH_4)_2$ by mild heating at 80°C in vacuum. MgB_2 was synthesized by reacting excess Mg with boron upon heating. X-ray diffraction (XRD) patterns confirming the high quality of our as-synthesized materials are shown in Figure 1, alongside patterns for the

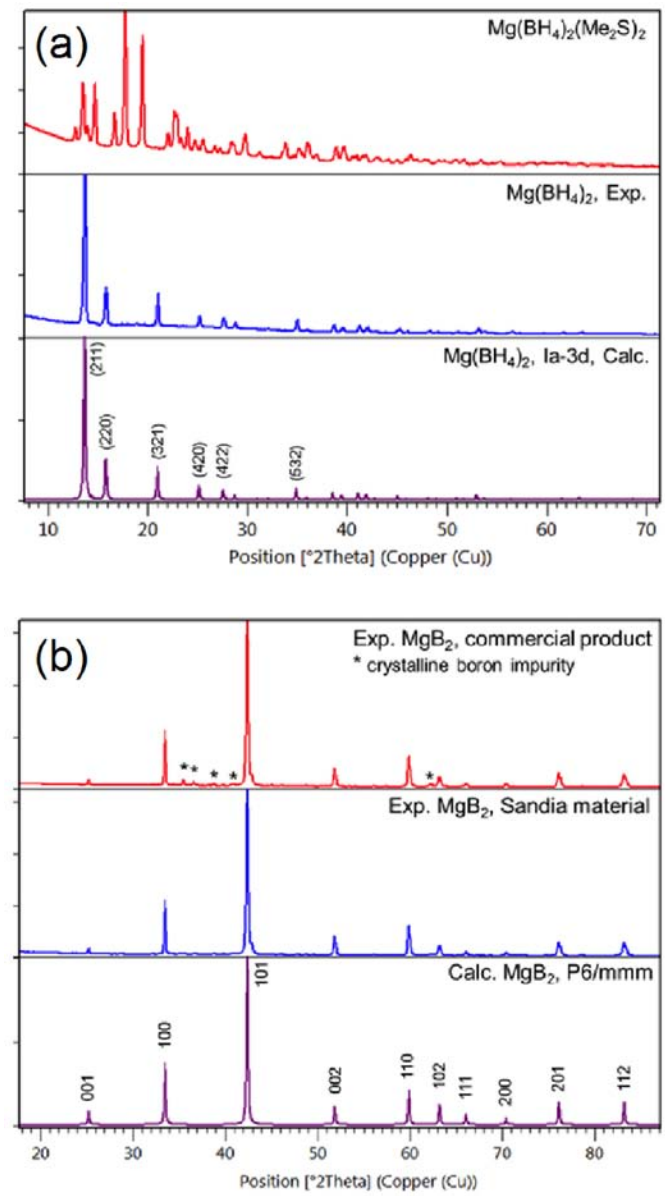

FIGURE 1. Synthesis of MgB_2 and $Mg(BH_4)_2$ (a) XRD patterns of as-synthesized $Mg(BH4)_2(SMe_2)_2$ and low temperature $Mg(BH_4)_2$ and a comparison with the calculated pattern for γ-$Mg(BH_4)_2$ (b) XRD pattern of high-purity MgB_2 synthesized at Sandia, compared with commercial MgB_2 and the calculated MgB_2 pattern

$Mg(BH_4)_2(SMe_2)_2$ precursor and commercial MgB_2 (found to contain significant crystalline boron impurities).

$Mg(BH_4)_2$ can be converted almost entirely to MgB_2 upon heating in vacuum up to 550°C, which involves several steps featuring formation of polyborate intermediates (e.g., $Mg(B_3H_8)$ and $MgB_{12}H_{12}$) alongside MgH_2 and Mg metal [4-9]. It has been further demonstrated that $Mg(BH_4)_2$ can be produced in good yield when MgB_2 is heated at 390–440°C and 70–90 MPa hydrogen pressure. However, in contrast to dehydrogenation, the composition and sequence of intermediates formed during MgB_2 rehydriding are poorly established. Such characterization is vital to understanding the hydrogenation pathway and the factors that control its kinetics. Accordingly, we collected hydrogenation data for bulk MgB_2 in a Seivert's instrument at several temperatures and at two different pressures (Figure 2). At 105 bar hydrogen pressure (Figure 2a), the uptake shows two distinct kinetic regions with ~0.02 wt%/h and 0.002 wt%/h hydrogenation kinetics (based on 105 bar hydrogen pressure and 380°C). The variable temperature (Figure 2b) studies allow a measurement of the activation energy (E_a) for hydrogenation within each of the identified kinetic regimes. Preliminary E_a values are 113 kJ/mol for the faster initial step and 191 kJ/mol for the slower second step. These numbers will be compared with theoretical estimates to identify the different rate limiting mechanisms.

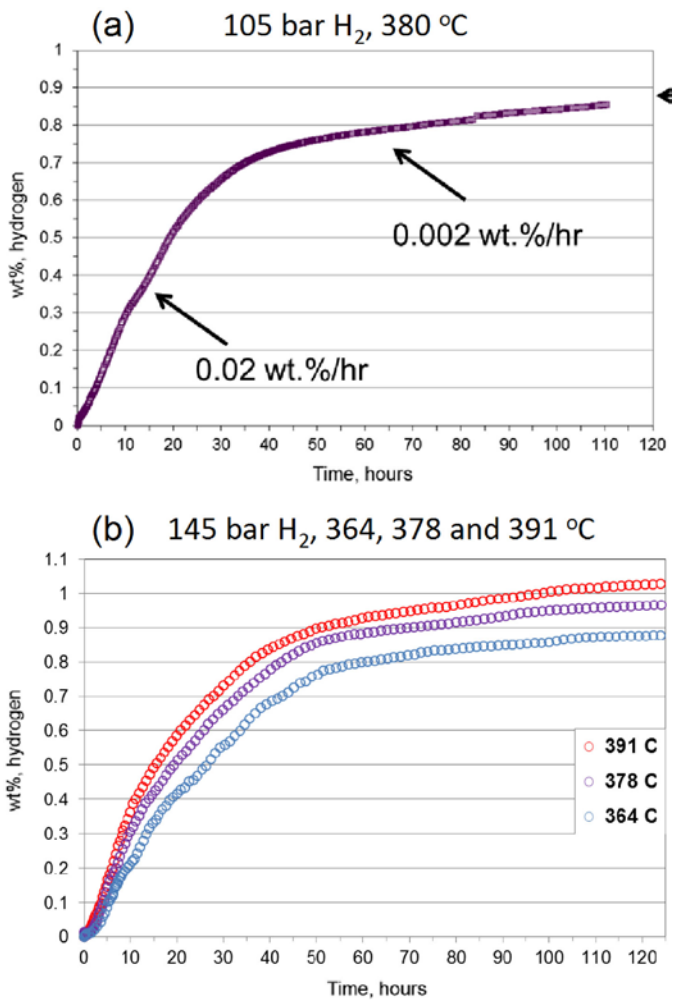

FIGURE 2. Hydrogenation kinetics of bulk MgB_2 (a) Hydrogenation at 105 bar of hydrogen at 380°C, highlighting two distinct kinetic regions with ~0.02 wt%/h and 0.002 wt%/h hydrogenation kinetics (b) Hydrogenation of bulk MgB_2 at 145 bar at 364°C, 378°C, and 391°C

Since intermediates may be present in amorphous phases or solid solutions, their identification requires methodologies beyond XRD that are chemically sensitive. Toward this end, we have collected XAS and XES spectroscopic data for MgB_2, $MgB_{12}H_{12}$, $Mg(BH_4)_2$, and samples at intermediate hydrogenation stages using the Lawrence Berkeley National Laboratory Advanced Light Source synchrotron. The XES data, along with appropriate reference spectra, are presented in Figure 3a. For these spectra, a B 1 s (K edge) core electron is ejected, and the resulting radiative decay of valence electrons into the core hole is measured as a function of emitted photon energy (specifically, we probe the *p*-component of the valence density of states due to dipole selection rules). The XES and XAS data are compared with theoretical simulations of some of the spectra in Figure 3a using the method described by Prendergast, et al. [10] (relative peak positions are typically reproduced better than amplitudes). In the experimental XES spectrum for MgB_2, there exists a main peak near 184 eV with a shoulder extending to 185.5 eV, as well as a poorly resolved shoulder at ~181 eV. All of these features also appear in the simulated spectra. In the experimental XES spectrum for pure $Mg(BH_4)_2$, we notice a wide peak centered around 181.0 eV as well as a smaller feature at around 193.5 eV. The simulated spectra reproduce the positions of both features well, confirming identification of these peaks. There is however a peak in the $Mg(BH_4)_2$ experimental spectrum at 184 eV which seems not to have a theory counterpart. This discrepancy is under examination. The $MgB_{12}H_{12}$ XES spectrum has a peak at 184 eV and a distinct shoulder at 187.5 eV. Calculated spectra for $MgB_{12}H_{12}$ are in progress, but the 187.5 eV peak, having no correspondence in the spectra of the other species, is useful in identifying $MgB_{12}H_{12}$ among the possible hydrogenation intermediates. B_2O_3 exhibits an XES spectrum similar to $Mg(BH_4)_2$, preventing unequivocal identification of oxidation based on XES alone; however, the XAS results (not shown here) do not exhibit features that are consistent with significant oxidation. Similar analyses of other potential reaction intermediates are underway, including simulations of spectra arising from different local coordinations and off-stoichiometric hydrogen compositions.

While analysis of the data is still in progress, some general conclusions can be drawn from the XES data in Figure 3. MgB_2 + H (1.2%, 391°C) and MgB_2 + H (0.8%, 380°C) exhibit spectra similar to as-prepared MgB_2, suggesting these samples at the early stages

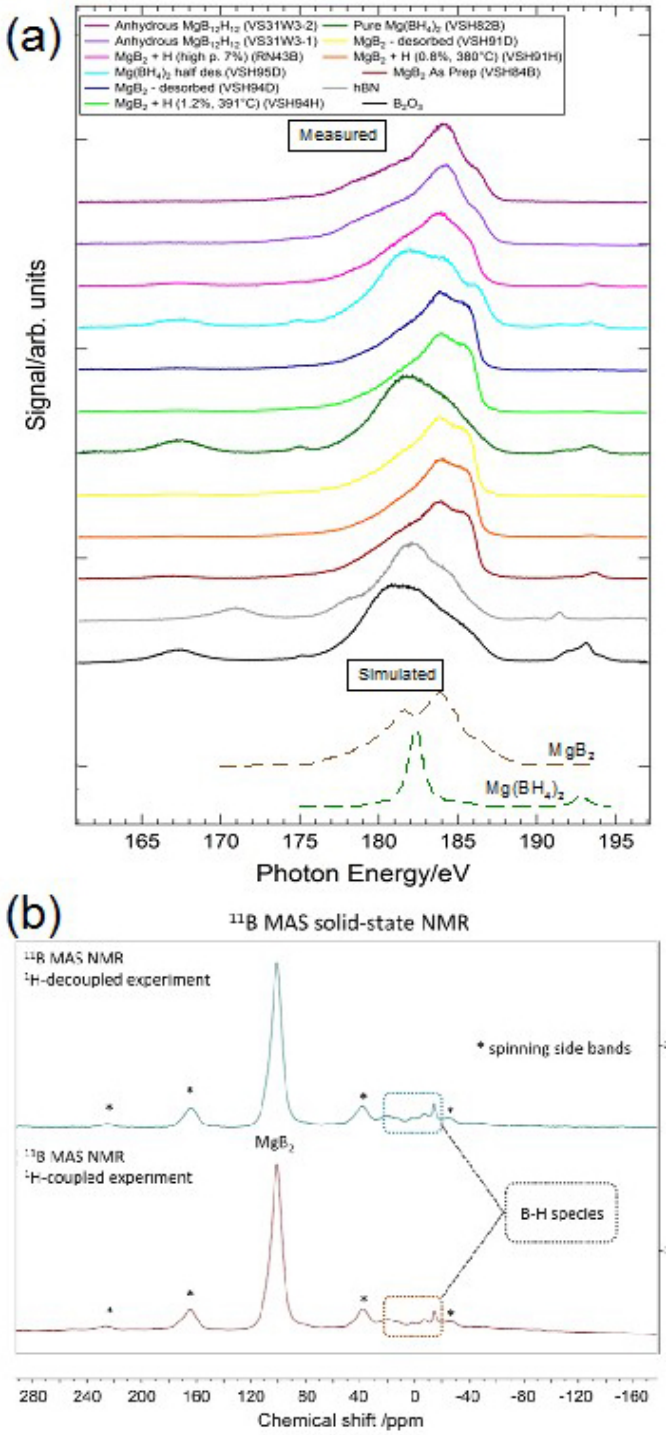

FIGURE 3. Spectroscopic characterization (a) Measured X-ray B K-edge XES spectra of anhydrous $MgB_{12}H_{12}$, pure $Mg(BH_4)_2$, MgB_2 produced by desorption, MgB_2 + H (high p. 7%), MgB_2 + H (0.8%, 380°C), $Mg(BH_4)_2$ half desorbed, MgB_2 as prepared, MgB_2 + H (1.2%, 391°C), hexagonal BN, and B_2O_3 samples, compared with theoretically simulated spectra for MgB_2 and $Mg(BH_4)_2$ (b) ^{11}B MAS spectra for a partially hydrogenated MgB_2 sample with 0.8 wt% H obtained from hydrogenation of MgB_2 at 364°C

of hydrogenation are retaining much of their original chemistry. The XES spectra for the half-desorbed (VSH95D) and half-hydrogenated (RN43B) $Mg(BH_4)_2$ are very different, indicating different pathways for desorption and hydrogenation. The half-desorbed sample looks like a mixture of the phase-pure $Mg(BH_4)_2$ and $MgB_{12}H_{12}$ spectra, whereas the half-hydrogenated sample more closely resembles the MgB_2 spectrum with little evidence for the formation of $MgB_{12}H_{12}$ or $Mg(BH_4)_2$. One feature of note in the XAS spectrum of partially hydrogenated MgB_2 is that the more bulk-sensitive (~100 nm) fluorescence yield shows very similar characteristics as the more surface-sensitive electron yield measurement (~1 nm sensitivity, not shown), which suggests that boron is being hydrogenated throughout the sample rather than just at the surface. Accordingly, hydrogen transport into the sample may not be as difficult as has generally been envisioned.

To gain further chemical sensitivity as a companion to the XAS/XES data, we also collaborated with Pacific Northwest National Laboratory to perform NMR measurements on our sample sets. The ^{11}B magic angle spinning (MAS) NMR spectra (Figure 3b) shows a spectrum of MgB_2 hydrogenated with 0.8 wt% H at 364°C. The results indicate that MgB_2 is the major species present (peak at ~100 ppm), however small amounts of B-H species are observed as well between -2 and -18 ppm. Although the identity of these species remains to be established, it is clear that at least some boron atoms in MgB_2 react with H_2 to form B-H bonds. Interestingly, no peaks from BH_4^- anions could be detected, suggesting the absence of $Mg(BH_4)_2$ material. This is consistent with the XES observations.

Theoretical: Significant progress was made in developing and parameterizing our software codes for predicting the thermodynamic and kinetic evolution of metal hydrides during (de)hydrogenation. Existing codes were adapted to account for thermodynamic hydrogenation conditions of temperature and partial pressure, and a formalism was included for studying the coexistence of multiple phases, including reaction intermediates. Two codes are being developed, (1) a code for predicting thermodynamic phase fractions of mixed-phase systems within a given microstructure, and (2) a code for predicting phase evolution kinetics using a PFM formalism. Both are intended to go beyond idealized descriptions based on bulk enthalpies alone and instead consider the complexities associated with surfaces and interfaces.

Our first code relies on DFT-computed bulk, surface, and interface energies, as well as zero-point and vibrational entropic contributions, to predict thermodynamic phase fractions based on an input microstructure. To account for microstructure-associated effects that are neglected in typical phase diagrams, we include penalties associated with the presence of surfaces and internal phase boundaries, as well as entropic contributions associated with phase

coexistence (assuming ideal mixing). Currently, only core-shell microstructures are implemented, although the framework is extensible. Pending delineation of the phase microstructure of the Mg-B-H system, this code was tested on the $Li_3N/LiNH_2$+2LiH system, which exhibits many properties in common with $MgB_2/Mg(BH_4)_2$ but has few intermediates and a core-shell phase microstructure that can be readily assumed from available literature data (Figure 4a). As a validating case, we focused on predicting two peculiar behaviors associated with nanosizing that were found in extensive (de)hydrogenation data collected previously by our Sandia partners: first, a transition from the low-pressure α-Li_3N phase to a high-pressure β-Li_3N phase; and second, a conversion from a two step reaction to a single-step reaction that eliminates the otherwise stable Li_2NH intermediate, resulting in dramatically improved kinetics and reversibility. Our computational framework was able to properly predict the α-Li_3N/β-Li_3N phase stability reversal for particles smaller than 7.1 nm diameter, driven by a larger surface energy penalty for α-Li_3N. On the other hand, the single step reaction cannot be explained by considering surface energies alone. Instead, by estimating interface energies within the assumed phase microstructure using an established empirical procedure [11], our framework predicts near-complete elimination of the ordinarily stable Li_2NH intermediate once the size is reduced beyond ~5 nm (Figure 4b–d). This further validates the predictive capability of the code and provides a concrete explanation for the experimentally

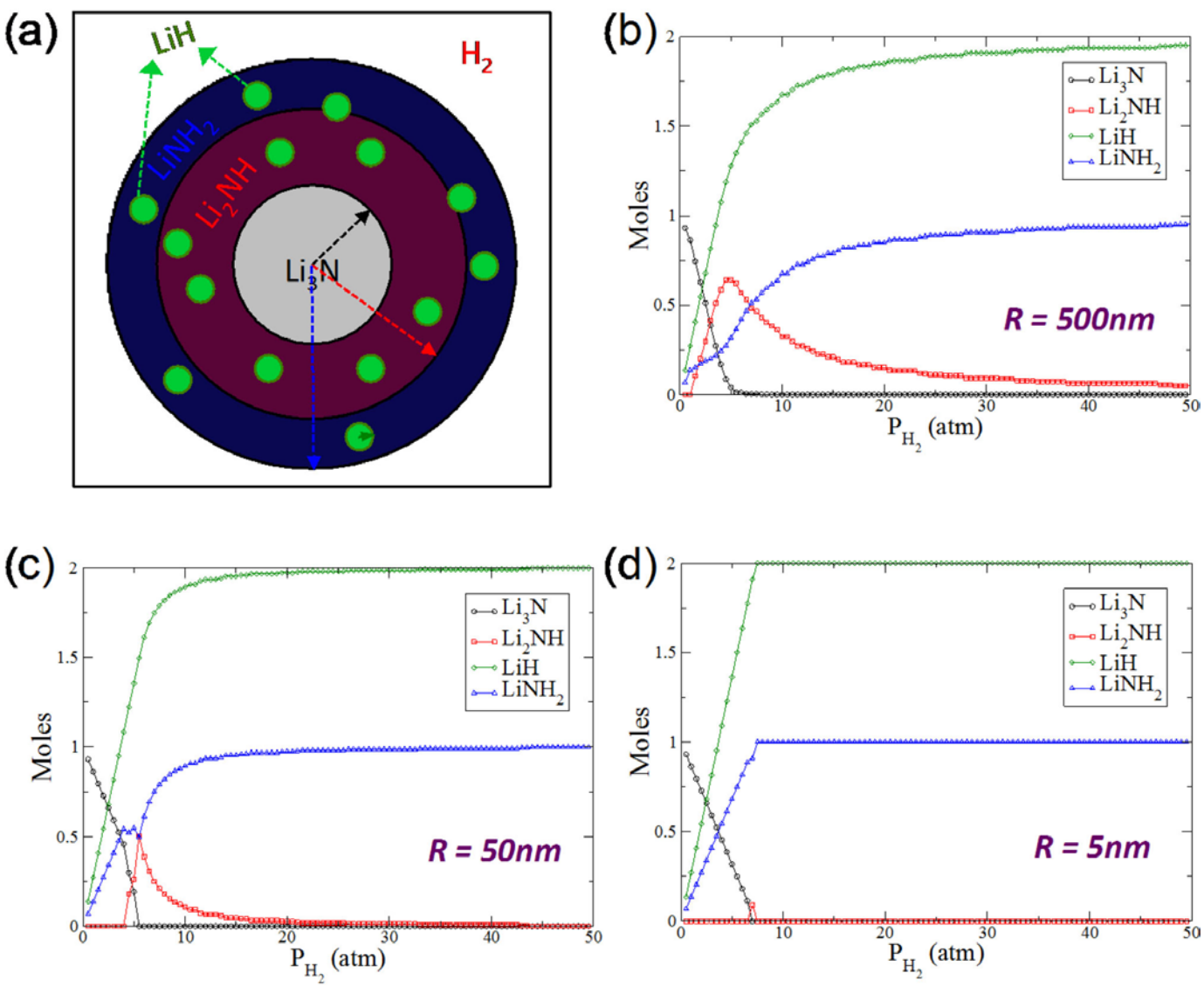

FIGURE 4. Predicted phase fractions in metal hydride nanoparticles (a) Core-shell model of the Li-N-H hydrogen storage system under hydrogenation conditions (b-d) Equilibrium phase fractions of Li_3N, Li_2NH, LiH, and $LiNH_2$ during hydrogenation for (a) 500 nm, (b) 50 nm, and (c) 5 nm radius particles. The smallest particles show essentially no evidence of stable Li_2NH intermediate formation (red)

observed single-step decomposition reaction. We emphasize that the disappearance of the intermediate results directly from the penalty associated with the formation of interfaces *within* the particle, which become increasingly larger contributions as the particle size is reduced. The possibility of using interfaces and phase microstructure to drive reaction pathways and kinetics is very compelling, and will be a key ingredient in our $Mg(BH_4)_2$ study. The results of this joint theory-experiment study have recently been submitted for publication [12].

Having established the predictive capability of the phase fraction code, we are currently obtaining the necessary parameters for application to the Mg-B-H system once the phase microstructure can be confirmed. In addition to previously calculated bulk enthalpies [4,7,9], we have computed the DFT energies for the low-index surfaces of MgB_2 and $Mg(BH_4)_2$, as shown in Table 1. We considered only (100) surfaces for $Mg(BH_4)_2$ because it neatly cleaves the large-scale arrangement of Mg atoms. The (100) surface of MgB_2 is the most stable, although (110) and (101) have surface energies that are within 20% of (100). $Mg(BH_4)_2$ has much lower surface energy, which could have important consequences for phase stabilities of nanostructured Mg-B-H systems. We are currently computing similar quantities for the possible intermediate phases, as well as elastic moduli for each phase that can be used to estimate contributions to interfacial energies arising from lattice mismatch at internal phase boundaries.

TABLE 1. DFT-computed surface energies (J/m^2) of low-index surfaces of $MgB_2/Mg(BH_4)_2$

Surface	MgB_2	$Mg(BH_4)_2$
(100)	1.92	0.32
(001)	2.72	--
(110)	2.24	--
(101)	2.24	--
(111)	2.56	--

The second code in our suite is designed to predict the kinetics of phase evolution, which will be an increasingly important effort in future project years. We are currently implementing formalisms for kinetic contributions arising from chemomechanical gradients based on differences in elastic moduli, non-equilibrium mass transport of hydrogen and metal cations, and phase nucleation barriers. These functionalities will be tested in the coming months. Explicit modeling of surface hydrogen dissociation and association will be performed via subcontract with the University of Michigan; this feature will be important for considering the effects of catalytic additives. Early versions of the PFM code using sample parameters have already been benchmarked on the high performance computing resources at LLNL. Both spherical and plate-shaped geometries were tested to ensure robustness against particle morphology. We were able to simulate the phase evolution upon 50% (de)hydrogenation of a model ~100 nm particle using an allocation of 160 central processing unit cores, running for one week of continuous processing time (~25,600 core-hours). We expect that further optimization may be possible. Corresponding parameters are currently being computed for the Mg-B-H using DFT and ab initio molecular dynamics.

CONCLUSIONS AND FUTURE DIRECTIONS

- Hydrogenation of MgB_2 evidences two distinct kinetic regimes. XAS/XES and NMR can uniquely identify BH_x chemical species at partial hydrogenation stages, and suggest that dehydrogenation and hydrogenation occur via different pathways.
- Phase fraction prediction code reproduces known reaction pathways in a complex metal hydride system. Early learning on the metal hydride system demonstrates the need to consider interfaces and suggests the possibility of morphological/microstructural engineering as a strategy for kinetic improvement.
- *Future direction:* Collect XAS/XES and Fourier transform infrared data and simulate corresponding theoretical spectra for additional samples of Mg-B-H at varying stages of (de)hydrogenation to get information on local chemical environments.
- *Future direction:* Establish the nanoparticle synthesis laboratory to begin the synthesis of MgB_2 and $Mg(BH_4)_2$ nanoparticles with controlled sizes.
- *Future direction*: Calculate remaining thermodynamic parameters for MgB_2, $Mg(BH_4)_2$, and $MgB_{12}H_{12}$ bulk, surfaces, and interfaces, comparing against literature values to benchmark chosen parameters. Perform ab initio molecular dynamics of MgB_2, $Mg(BH_4)_2$, and key intermediates and surfaces for extraction of transport coefficients and anharmonic contributions to entropy.
- *Future direction*: Implement additional physical ingredients in our kinetics code, including a new modeling framework for chemical reaction kinetics on surfaces (clean or oxidized).

FY 2015 PUBLICATIONS/PRESENTATIONS

1. Wood, B.C. et al., "Improving the kinetics and thermodynamics of $Mg(BH_4)_2$ for hydrogen storage." *U.S. DOE Hydrogen and Fuel Cells Program Annual Merit Review*, Washington, D.C., June 2015.

2. Stavila, V., N. Poonyayant, T.-W. Heo, K. Ray, T.J. Udovic, N. Angboonpong, P. Pakawatpanurut, L.E. Klebanoff, B.C. Wood, "Nanostructuring: A Route for Enhancing Reversibility in Metal Hydrides?" *Gordon Conference on Hydrogen-Metal Systems*, Easton, MA, July 2015.

3. Wood, B.C., V. Stavila, N. Poonyayant, T.-W. Heo, K. Ray, L.E. Klebanoff, T.J. Udovic, J. Lee, N. Angboonpong, and P. Pakawatpanurut, "Nanointerface-driven reversible hydrogen storage in the nanoconfined Li-N-H system." *Submitted* (2015).

REFERENCES

1. Klebanoff, L. E., and J.O. Keller, "5 Years of Hydrogen Storage Research in the US DOE Metal Hydride Center of Excellence (MHCoE)," *Int. J. Hydr. Energy* 38 (2013): 4533-4576.

2. Pasini, J.M., C. Corgnale, B.A. van Hassel, T. Motyka, S. Kumar, and K.L. Simmons, "Metal Hydride Material Requirements for Automotive Hydrogen Storage Systems," *Int. J. Hydr. Energy* 38 (2013): 9755-9765.

3. Fichtner, M., Z. Zhao-Karger, J. Hu, A. Roth, and P. Weidler, "The Kinetic Properties of $Mg(BH_4)_2$ Infiltrated in Activated Carbon," *Nanotechnology* 20 (2009): 204029.

4. Zhang, Y., E. Majzoub, V. Ozoliņš, and C. Wolverton, "Theoretical Prediction of Metastable Intermediates in the Decomposition of $Mg(BH_4)_2$," *J. Phys. Chem. C* 116 (2012): 10522-10528.

5. Chong, M., A. Karkamkar, T. Autrey, S. Orimo, S. Jalisatgi, and C.M. Jensen, "Reversible Dehydrogenation of Magnesium Borohydride to Magnesium Triborane in the Solid State Under Moderate Conditions." *Chem. Commun.* 47 (2011): 1330-1332.

6. Hwang, S.-J., R.C. Bowman, J.W. Reiter, J. Rijssenbeek, G.L. Soloveichik, J.-C. Zhao, H. Kabbour, and C.C. Ahn. "NMR Confirmation for Formation of $[B_{12}H_{12}]^{2-}$ Complexes during Hydrogen Desorption from Metal Borohydrides." *J. Phys. Chem. C* 112 (2008): 3164-3169.

7. Ozolins, V., E.H. Majzoub, and C. Wolverton, "First-Principles Prediction of Thermodynamically Reversible Hydrogen Storage Reactions in the Li-Mg-Ca-BH System," *J. Am. Chem. Soc.* 131 (2008): 230-237.

8. Soloveichik, G.L., Y. Gao, J. Rijssenbeek, M. Andrus, S. Kniajanski, R.C. Bowman, S.-J. Hwang, and J.-C. Zhao, "Magnesium Borohydride as a Hydrogen Storage Material: Properties and Dehydrogenation Pathway of Unsolvated $Mg(BH_4)_2$," *Int. J. Hydr. Energy* 34 (2009): 916-928.

9. Zhang, Y., E. Majzoub, V. Ozoliņš, and C. Wolverton, "Theoretical Prediction of Different Decomposition Paths for $Ca(BH_4)_2$ and $Mg(BH_4)_2$," *Phys. Rev. B* 82 (2010): 174107.

10. Prendergast, D., and G. Galli, "X-ray absorption spectra of water from first principles calculations," *Phys. Rev. Lett.* 96 (2006): 215502.

11. Porter, D.A., and K.E. Easterling, *Phase Transformations in Metals and Alloys.* 2nd ed.; Chapman & Hall: London, UK (1992).

12. Wood, B.C., V. Stavila, N. Poonyayant, T.-W. Heo, K. Ray, L.E. Klebanoff, T.J. Udovic, J. Lee, N. Angboonpong, and P. Pakawatpanurut, "Nanointerface-Driven Reversible Hydrogen Storage in the Nanoconfined Li-N-H System," *submitted* (2015).